

Won-Suk Kim · Mira Park · Dai Woon Lee
Myeong Hee Moon · Heungbin Lim · Seungho Lee

Size-based analysis of incinerator fly ash using gravitational SPLITT fractionation, sedimentation field-flow fractionation, and inductively coupled plasma-atomic emission spectroscopy

Received: 2 July 2003 / Revised: 7 October 2003 / Accepted: 14 October 2003 / Published online: 20 December 2003
© Springer-Verlag 2003

Abstract Fly ash has been regarded as hazardous because of its high adsorption of toxic organic and/or inorganic pollutants. Fly ash is also known to have broad distributions of different chemical and physical properties, such as size and density. In this study, fly ash emitted from a solid waste incinerator was pre-fractionated into six sub-populations by use of gravitational SPLITT fractionation (GSF). The GSF fractions were then analyzed by sedimentation field-flow fractionation (SdFFF) and ICP–AES. SdFFF analysis showed the fly ash has a broad size distribution ranging from a few nanometers up to about 50 μm . SdFFF results were confirmed by electron microscopy. Inductively coupled plasma–atomic emission spectroscopy (ICP–AES) analysis of the GSF fractions showed the fly-ash particles contain a variety of inorganic elements including Ca, Si, Mg, Fe, and Pb. The most abundant in fly ash was Ca, followed by Si then Mg. No correlations were found between trace element concentration and particle size.

Keywords Incinerator fly ash · Inorganic elements · Inductively coupled plasma–atomic emission spectroscopy · Sedimentation field-flow fractionation · Size distribution · SPLITT fractionation

W.-S. Kim · M. Park · D. W. Lee
Department of Chemistry, Yonsei University,
120-749 Seoul, Korea

M. H. Moon
Department of Chemistry, Pusan National University,
609-735 Pusan, Korea

H. Lim
Department of Chemistry, Dankook University,
140-714 Seoul, Korea

S. Lee (✉)
Department of Chemistry, Hannam University,
306-791 Taejeon, Korea
e-mail: slee@hannam.ac.kr

Present address:

W. Kim
Department of Chemistry and the Beckman Institute,
University of Illinois, Urbana, Illinois 61801, USA

Introduction

Most of the waste generated by modern society is treated in waste-incinerators and then land-filled. It has been reported that in 1994 over 306 million tons of municipal solid waste (MSW) was generated and incinerated in the United States alone and that amount is increasing by roughly 5% annually [1]. However, in many countries this situation is likely to change as suitable landfill sites become less available and the regulations on waste-dumping become increasingly stringent. Although incineration greatly reduces the volume of the waste, it still leaves a considerable amount of solid residue in the form of fly ash [2]. Fly ash is composed of particles of various sizes ranging from less than a nanometer up to a few micrometers [3, 4, 5]. Fly-ash particles frequently contain toxic species such as heavy metals and persistent organic compounds (e.g. PAH, PCB and PCDD) which are easily leached into the environment because of the high surface area-to-mass ratio [6, 7, 8]. It has been also reported that there is a close relationship between the particle size of fly ash and the quantity and/or composition of the heavy metal contaminants [3, 9, 10]. Thus accurate determinations of the size and size distribution of fly-ash particles are important in controlling and tracing the fate of pollutants.

Due to increasing concern over the environmental impact of the fly-ash particles, development of a rapid, convenient, and size-specific analytical method is required. Accurate size analysis of fly-ash particles is not simple due to its heterogeneous and polydisperse nature with regard to physical properties [11] such as size, density, mass, and shape. As a result, there have not yet been many studies reported on analysis of the size of fly ash [10, 11, 12].

Various sizing techniques have been developed and used for environmental particles, including the Coulter multisizer [5, 12, 13, 14], the scanning mobility particle sizer (SMPS) [15, 16, 17], aerosol time-of-flight mass spectroscopy (ATOFMS) [18, 19], microscopy [16, 20, 21], and photon correlation spectroscopy (PCS) [22, 23, 24]. All these methods have their own advantages and disadvantages in terms of analysis time, sensitivity, and cost, etc. [21, 23, 25].

Sedimentation field-flow fractionation (SdFFF) is a particle sizing technique which provides size-based separation of particles. SdFFF has been used for separation and sizing of a variety of particulate samples including environmental particles [12, 25, 26, 27]. The potential of SdFFF for size-analysis of incinerator fly ash has already been reported [12]. There are two main elution mechanisms in sedimentation FFF, “normal” and “steric”. In the normal mode retention depends on the diffusion coefficient of the sample. Particles having a higher diffusion coefficient (smaller particles) form a layer of greater thickness (more diffusive) and are eluted earlier than particles having lower diffusion coefficients (larger particles). In the normal mode the effective mass of the sample can be directly determined from its retention time. Particle size can then be determined from the effective mass. The normal mode is applicable to particle diameters extending from 1 or 2 μm down to about 1 nm.

As particle size increases a point is reached after which the particle size becomes greater than the mean layer thickness, which results in an elution order reversed from that of the normal mode – larger particles are eluted earlier than smaller ones. This mode, applicable generally to particles larger than about 1 μm , is termed “steric” mode”. Unlike in the normal mode, particle size cannot be obtained directly from the retention time in the steric mode of SdFFF and thus a calibration is generally required. The steric mode of SdFFF (Sd/StFFF) is particularly useful for fast separation (usually within 10 min) and for sizing of particles larger than about 1 μm [28, 29, 30].

SPLITT fractionation (SF) has been developed into a useful tool for fractionation of particulate samples with broad size distributions into fractions with narrower size distributions, including environmental samples [31, 32, 33]. SF has advantages over particle-fractionation methods such as membrane filtration and static sedimentation in that the samples are not subjected to high mechanical stress during SF separation. Also, SF has a well-constructed theoretical basis and thus separation parameters (e.g. cut-off diameter) can be easily controlled by adjusting the flow rates or if necessary the applied field strength. Finally, SF is usually fast and can be operated continuously, enabling large samples to be fractionated. Recently, a particle concentrator using an upstream ultrafiltration (PCUU) system [31] was developed for SF, which enabled on-line sample concentration during a continuous SF operation.

The goal of this study was to combine SF and SdFFF for accurate size analysis of fly ash. Fly ash collected from a municipal solid waste incinerator would first be separated into several sub-populations using gravitational SF (GSF), an SF technique that uses gravity as the external field. The GSF fractions would then be analyzed for size and elemental composition using SdFFF and ICP–AES, respectively.

Experimental

Samples

Polystyrene latex beads obtained from Duke Scientific (Palo Alto, CA, USA) were used as particle-size standards. The latex beads were diluted with the carrier liquid 100–200 times to prepare standard mixtures. The fly ash samples were provided by Dr Y.S. Chang of the School of Environmental Engineering, Pohang University of Science and Technology and had been collected using a bag filter from a municipal solid waste incinerator in Changwon, South Korea, in August, 2000. The fly-ash particles were recovered from the bag filter and then suspended in water containing 0.1% FL-70. The aqueous suspension of the fly-ash particles was then passed through a 270-mesh sieve ($\sim 53 \mu\text{m}$ pore size) to remove large impurities and any particles larger than about 50 μm . The samples were then dried and stored for SF fractionation. The density of the fly-ash particles, measured using a specific gravity bottle, was 2.5 g cm^{-3} . Coal fly ash (CRM 1633b, NIST, USA) was used as the standard material for the recovery test in the ICP–AES analysis.

Gravitational SPLITT fractionation

Four GSF channels of different dimensions were used for fractionation of the fly-ash particles. The four channels had the dimensions b (breadth) $\times L$ (length) 2 \times 5, 3 \times 15, 4 \times 20, and 6 \times 20 cm, and were used for the theoretical cut-off diameters of 20, 10, 5, and 2.5 (and 1.0) μm , respectively. All four channels had a similar 360 μm thickness (2 \times 130 μm -thick Mylar spacers+1 \times 100 μm -thick stainless steel plate). Approximately 20 g of the dried fly ash was added into the carrier liquid (water containing 0.02% NaN_3) at a concentration of about 1.0% (w/v), and then sonicated for 1 h to prepare a suspension of the fly ash. The aqueous suspension of the fly ash was continuously fed into the top inlet of the GSF channel using a peristaltic pump (Gilson Minipulse 3, Villers-leVel, France), while the carrier was fed into the bottom inlet of the GSF channel using a FMI laboratory pump (Fluid Metering, Oysterbay, NY, USA). Detailed experimental procedures of GSF fractionation of fly ash have been described elsewhere [31, 33].

Sedimentation field-flow fractionation

The SdFFF system used was a model S101 colloid/particle fractionator purchased from Postnova USA (Salt Lake City, Utah). The channel was 0.0127 cm thick, 89.1 cm long, and 1.1 cm wide and the rotor radius was 15.1 cm. The channel void volume was measured from the elution volume of acetone and found to be 1.23 mL. The elution of particles was monitored by means of an M720 UV/VIS detector (Young-In Scientific, Seoul, Korea) at the fixed wavelength of 254 nm, and the detector signal was processed using the FFF software provided by Postnova.

Scanning electron microscopy

A Jeol model JSEM-5410LV (Tokyo, Japan) scanning electron microscope (SEM) was used with an acceleration potential of 20 kV. The fly-ash particles were mounted and fixed on a 0.1 μm Nucleopore filter and then sputter-coated with gold with a Hummer III sputter coater (Alexandria, VA, USA).

Inductively coupled plasma-atomic emission spectroscopy

A sequential ICP–AES with a nitrogen purge (Jovin-Yvon JY 138 Ultra trace, France), and equipped with a 40.68-MHz RF generator with a demountable standard torch and a 1-m focal length monochromator was used to determine the concentration of metals in the

fly-ash particles. The instrument was operated at a forward power of 1.1 kW and with a coolant gas flow of 14 L min⁻¹. The sheath gas was used for analysis of Na only. The sample solutions were introduced into a PFA nebulizer (μ flow PFA-100, Elemental Scientific, USA) at an uptake rate of 100 μ L min⁻¹ using a peristaltic pump (Gilson Minipulse 3, Villers-leVel, France); a Scott-type spray chamber was used. The selected wavelengths for Ca, Si, Mg, Fe, Pb, Ba, Cr, and Ni were 396.847 nm, 212.412 nm, 280.270 nm, 238.204 nm, 216.999 nm, 493.409 nm, 205.552 nm, and Ni: 232.003 nm, respectively.

For alkali fusion approximately 0.1 g dried fly ash was transferred into a Pt crucible (No. 20), and then 0.5 g boric acid (Analytical grade, Aldrich, Milwaukee, USA) and 1.5 g sodium carbonate (Duksan Pharmaceutical, Korea) was added. The fused sample was then dissolved in 20 mL 1:1 (v/v) HCl solution in water (Semiconductor grade, Dong Woo Pure Chemical, Iksan, Korea) and transferred into a 100-mL polyethylene volumetric flask. Standard metal solutions were prepared from 1000 μ g mL⁻¹ spectroscopic standards (NIST CRM). A 10 ppm (μ g mL⁻¹) Mg solution was used to optimize the system. All calibrations were carried out by the standard addition method.

Results and discussion

Gravitational SPLITT fractionation of fly ash

Details of the procedure and results of GSF fractionation of fly ash have been published elsewhere [33]. Six fractions of fly ash were obtained from the four GSF channels operating at theoretical cut-off diameters of 1.0, 2.5, 5, 10, and 20 μ m and were named “SF-1” to “SF-6”. Theoretically SF-1 should have contained particles having diameters smaller than 1.0 μ m, SF-2 between 1 and 2.5 μ m, SF-3 between 2.5 and 5 μ m, SF-4 between 5 and 10 μ m, SF-5 between 10 and 20 μ m, and SF-6 between 20 and 53 μ m. Size analysis of each fraction by optical and electron microscopy showed reasonable agreement with theory [33]. For on-line concentration of the fractionated particles PCUU were employed [31, 33]. The concentrated fractions were then dried in an oven for 2 h before SdFFF analysis.

Separation by SdFFF in normal mode

A mixture of four submicron-sized polystyrene latex beads (222, 343, 502, 705 nm) was well separated by the normal mode of SdFFF (Sd/NIFFF) in water containing 0.1% FL-70 and 0.02% NaN₃ (data not shown). Field-programming [34] was used in which the field strength (i.e. channel rotation rate) was gradually decreased according to a power function during the SdFFF run. Field-programming is typically used to avoid excessive retention of larger components and to improve their detectability. The programming settings were initial and final field strengths of 1850 and 75 rpm, respectively, pre-decay time of 5 min, and t_a of -40. The flow rate was 1.1 mL min⁻¹. As mentioned earlier, the particle diameter can be directly determined from the retention time in Sd/NIFFF [26, 35]. The measured diameters are in good agreements with the nominal diameters within a relative error of about 5% (data not shown).

Separation by SdFFF in steric mode

As described previously, larger particles are eluted earlier than smaller ones in the steric mode of SdFFF (Sd/StFFF) [36]. The result shows a mixture of ten micron-sized polystyrene latex beads (40, 30, 20, 15, 10, 7, 5, 4, 3, 2 μ m) was separated well (data not shown). The field strength and flow rate were held constant at 1850 rpm and at 5.58 mL min⁻¹, respectively. The high resolution of the steric mode enabled use of a high flow rate, and a good separation was obtained within about 7 min. The carrier liquid was 1.0% FL-70 with no sodium azide added. This time, the sodium azide was not added and the concentration of FL-70 was 1% instead of 0.1%. The resolution seemed to be better at 1% than 0.1% FL-70 (although the difference was not significant), and the presence of sodium azide did not make any difference to the separation.

A calibration plot of log (retention time) versus log (diameter) was obtained from the retention data for each polystyrene particle size (data not shown). The results show linearity is excellent with a correlation coefficient, R^2 , of 0.9992. The absolute value of the slope of the calibration plot, which is called “size-based selectivity (S_d)” in FFF, is 0.747. This calibration plot can be used for determination of size and size distribution of the fly-ash particles using Sd/StFFF.

Sedimentation field flow fractionation of fly ash

SdFFF was employed for accurate size analysis of the six GSF fractions. Figure 1A shows a Sd/NIFFF fractogram of the SF-1 fraction. Elution of the sample was complete within about 50 min. Field-programming was not used this time to prevent loss of fractionation power. As described earlier, a fractogram obtained by Sd/NIFFF can be directly transformed to a size distribution. Figure 1B shows that the size distribution of SF-1, obtained from the fractogram shown in Fig. 1A, ranges from about 0.2 to about 0.45 μ m.

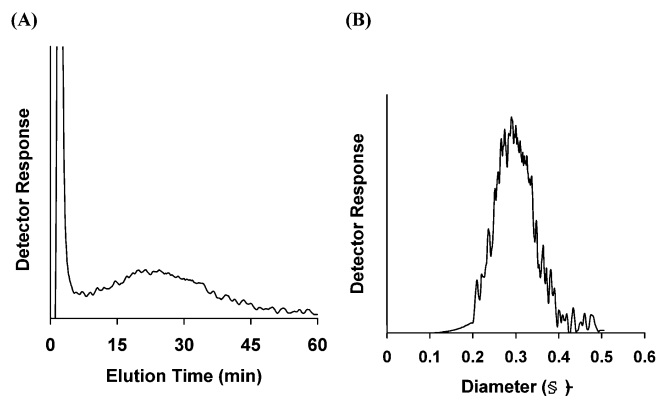


Fig. 1 Sd/NIFFF fractogram (A) and size distribution (B) of SF-1. The field strength was 650 rpm. The carrier liquid was water containing 0.1% FL-70 and 0.02% NaN₃ and the flow rate was 1.1 mL min⁻¹

Size analysis of the SF-2 to SF-6 fractions was accomplished using the steric mode of SdFFF (Sd/StFFF). In Sd/StFFF a density compensation is required if the density of the sample is different from the calibration standards in order to normalize the sample and the calibration standards to the same effective field strength (i.e. centrifugal force) [37]. The centrifugal force is proportional to $(\sqrt{\Delta\rho} \cdot \text{rpm})$, where $\Delta\rho$ is the density difference between the carrier liquid and the sample. For density compensation, Eq. (1) must be met.

$$\left(\sqrt{\Delta\rho_{\text{standard}}} \cdot \text{rpm}_{\text{standard}}\right) = \left(\sqrt{\Delta\rho_{\text{sample}}} \cdot \text{rpm}_{\text{sample}}\right) \quad (1)$$

$\Delta\rho_{\text{standard}}$ is the density difference between the standard and the carrier liquid, and $\Delta\rho_{\text{sample}}$ is the density difference between the sample and the carrier liquid. $\text{rpm}_{\text{standard}}$ and $\text{rpm}_{\text{sample}}$ are the field strengths used for calibration and for sample analysis, respectively. When $\Delta\rho_{\text{standard}}$, $\text{rpm}_{\text{standard}}$, and $\Delta\rho_{\text{sample}}$ are known, the channel rotation rate to be used for sample analysis ($\text{rpm}_{\text{sample}}$) can be calculated from Eq. (1). In this study, the calibration plot was prepared using polystyrene latex beads (density=1.05 g mL⁻¹) in an

aqueous carrier (density=1.00 g mL⁻¹) at a channel rotation rate of 1850 rpm. Thus the channel rotation rate for the analysis of fly ash (density=2.5 g mL⁻¹) has to be 340 rpm.

Figure 2 shows Sd/StFFF fractograms of the SF-2 to SF-6 fractions which were obtained under the same conditions as used for the separation of standards, except the field strength which was lowered to 340 rpm for density-compensation. According to SF theory the average particle size should gradually increase as the fraction number increases in the series SF-1 to SF-6. Because retention time (t_r) decreases as particle size increases in the steric mode of FFF, SF-6 was expected to be eluted first, followed by SF-5, and so on. As shown in Fig. 2, elution of fractions SF-4 to SF-6 follows Sd/StFFF theory (i.e. elution gradually shifts to higher retention as expected).

Interestingly, unlike fractions SF-4 to SF-6, SF-2 and SF-3 did not follow the elution order predicted by Sd/StFFF theory. Instead, SF-2 was eluted earlier than SF-3 and SF-3 earlier than SF-4. This would imply that the average size decreased in the order SF-2, SF-3, and SF-4. However, this was not in agreement with previously reported results [33]. The cause of this inconsistency is believed to be the contamination of the GSF fractions by submicron-sized particles, which behave as if they are in the normal mode (Sd/NIFFF).

In GSF separation is not based on size alone and provides a purely size-based separation only if all the particles have the same density. But, as mentioned earlier, fly ash contains particles with a broad range of densities, because of the various heavy metal and organic species present. In GSF separation of particles depends on their sedimentation coefficient, which is a measure of the sedimentation velocity of the particles [38]. The sedimentation coefficient is a function of $\Delta\rho \cdot d^2$, where $\Delta\rho$ is the density difference between the particles and the carrier liquid and d is the particle diameter. Thus, a given GSF fraction could contain different sized particles provided they have the same $\Delta\rho \cdot d^2$ value.

In SF-2, there is another possibility we may think. The particle diameter range obtained from GSF is expected to be 1.0–2.5 μm . However, some small particles (smaller than 1.0 μm) might have eluted in SF-2 fraction because of the incomplete initial transportation of particles toward the upper wall of the GSF channel. When suspended particles are introduced to the GSF channel, they must be transported against gravity to the upper channel wall by the high speed carrier flow stream entering from the lower inlet of GSF. At this stage efficient compression of particles by the carrier flow stream minimizes non-ideal behavior of initial particle trajectories. However, experimental flow rate condition used for the cut-off run of SF-2 fraction was very low – 0.4 mL min⁻¹ for feed rate and 0.8 mL min⁻¹ for carrier flow rate. With such a low carrier flow rate it is not sufficient to provide efficient and quick transportation of particles toward the upper wall. Some of the particles might therefore start migrating without being compressed near the upper wall. This deviation will lead to coelution

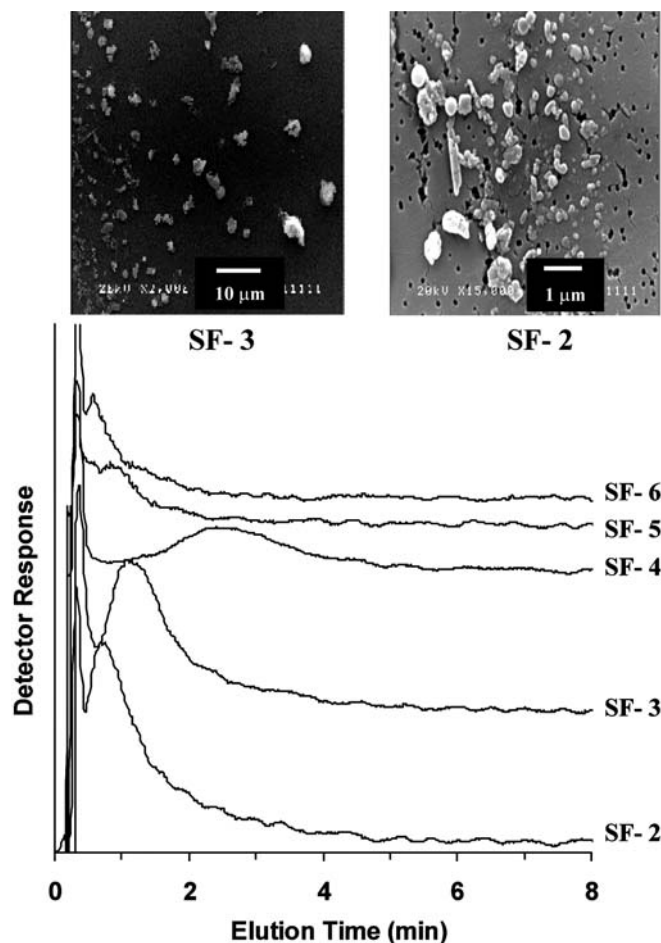


Fig. 2 Sd/StFFF fractograms of SF-2 to SF-6 and a scanning electron micrograph of SF-2 and SF-3. The field strength was 340 rpm, flow rate 5.6 mL min⁻¹, and the carrier liquid was water containing 1.0% FL-70

of small particles ($<1\ \mu\text{m}$) to both outlets. In this case, the number percentage of particles that belong to the expected diameter range at SF-2 was counted as approximately 60% which is comparatively lower than that of other fractions (around 80%).

Examination of fractions SF-2 and SF-3 by SEM at higher magnification confirmed the presence of submicron-sized particles (see the SEM pictures of SF-2 and SF-3 in Fig. 2). The presence of submicron-sized particles interferes with size analysis by Sd/StFFF, in that these particles behave as if they are in the normal mode of SdFFF (Sd/NIFFF) and thereby reverse the elution order. These small particles, even a small amount, can be a serious problem, because they usually give a higher detector response per unit mass than larger particles. Submicron-sized particles were observed in all GSF fractions. Although it was not accurately measured, the relative amount of these particles seemed to decrease as the fraction-number increased from SF-2 to SF-6 (data not shown). Almost no submicron-sized particles were found in SF-6. The deviations from the theoretical trend of the SF-2 and SF-3 fractions were probably because of a relatively larger contribution by the submicron-sized particles.

Elemental analysis of GSF fractions by ICP–AES

The GSF fractions of fly ash were analyzed for metal content by ICP–AES with the alkali fusion method. The alkali fusion method was first tested for its recovery using a standard material (NIST CRM), and the results are summarized in Table 1. For all the elements tested recoveries higher than 93% were obtained. Results from ICP–AES

Table 1 Recovery by alkali fusion method and ICP–AES for NIST CRM 1633b

Element	Theoretical value (mg kg ⁻¹)	Experimental value (mg kg ⁻¹)	Relative error (%)	Recovery (%)
Cr	198.00	188.0	5.1	95
Ba	120.50	110.5	8.3	95
Ca	15100	14000	7.3	93
Mg	4820.0	4600	4.6	95
Fe	7780.0	7250	6.8	93

Table 2 Metal concentrations in GSF-fractions of fly ash measured by ICP–AES

Element	Concentration (mg kg ⁻¹) in:					
	SF-1	SF-2	SF-3	SF-4	SF-5	SF-6
Ca	179000 (5.7)	194000 (2.1)	190000 (1.5)	217000 (5.8)	213000 (2.0)	178000 (0.4)
Si	34700 (2.2)	48300 (2.8)	44300 (4.2)	50600 (7.4)	60100 (3.2)	86800 (0.1)
Mg	25800 (3.0)	35900 (2.3)	27400 (1.0)	24300 (5.3)	17400 (6.2)	25500 (26)
Fe	9000 (3.2)	11300 (2.5)	10200 (1.9)	9400 (0.8)	14000 (1.5)	17300 (4.9)
Pb	10800 (5.3)	14400 (3.7)	13000 (4.9)	6730 (6.1)	5740 (2.5)	2930 (5.1)
Ba	830 (25)	860 (8.8)	1110 (4.9)	1210 (0.1)	1340 (5.4)	1640 (29)
Cr	450 (11)	530 (4.6)	470 (4.6)	320 (0.2)	360 (3.1)	490 (8.7)
Ni	62 (15)	61 (7.0)	68 (12)	70 (27)	59 (9.2)	115 (3.0)

Numbers in parenthesis are the relative standard deviation (%)

analysis of all GSF fractions are shown in Table 2 and also in Fig. 3. All GSF fractions had similar compositions with Ca being the most abundant element present, followed by Si, and then Mg. In addition, Fe and Pb were also found to be present but V, As, Se, and Hg were not detected.

In general, the surface area-to-mass ratio increases as particle size decreases, and thus the relative amount of species adsorbed on the surface of particles tends to increase with decreasing size [3, 6]. However, as shown in Fig. 3, no particular correlation was observed between metal concentration and the particle size. There are several possible reasons for this. First, elemental analysis was perturbed by inaccurate size fractions obtained from GSF. As shown in Fig. 2, some GSF fractions, especially fraction 2 and 3, contain submicron particles. However, we can easily see that this is not a critical reason, because GSF 1 also contains very small concentrations of inorganic elements. Second, if a volatilized element [39] does not undergo significant condensation, adsorption, or reaction with the fly ash surfaces, the difference in the degree of the element enrichment in the smallest and the largest particles might not be large, and the concentration of the elements would be nearly independent of particle size. In addition, the mechanism of particle formation in an incinerator is quite different for coal fly ash. Because the current work is mainly focused on demonstrating a combined analytical technique for determining the size-dependence of levels of toxic elements, a thorough examination has not been undertaken. Therefore, further studies of various types of fly ash sample are needed to obtain detailed information on dependence of patterns on particle size.

The aqueous medium of the fly ash suspension used for GSF fractionation was also analyzed using the same ICP–AES method and the results are summarized in Table 3. Unlike the fly-ash particles, Mg was the most abundant element in the suspension liquid. This indicates that a relatively higher proportion of the Mg was present as water-soluble compounds on the surface of the particles. Even so, the concentrations of Cr, Ba, and Mg were much lower in the suspension medium than in the particles and Si and Pb were not detected in the suspension medium. These results are consistent with an earlier report which found that Pb and Cr were generally present in fly ash as oxides and hydroxides rather than as chlorides, sulfides, or carbonates [40].

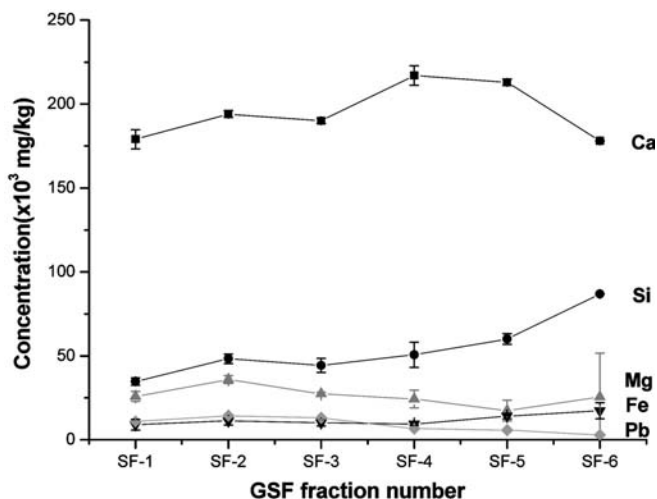


Fig. 3 Metal content of six GSF fractions of fly ash determined by ICP–AES

Table 3 Metal concentrations in the aqueous medium of fly ash suspension measured by ICP–AES

Element	Concentration (mg kg ⁻¹)	Relative standard deviation (%)
Mg	1610	3.8
Ca	109	2.6
Fe	109	3.4
Ba	78	7.1
Cr	23	5.4
Pb	<53	–
Ni	<45	–
Si	<40	–

Conclusions

A combination of GSF, SdFFF, and ICP–AES is a useful tool for analysis of fly-ash particles generated by solid waste incinerators. In particular, GSF is useful for pre-fractionation of the fly-ash particles into a few subpopulations having narrower size distributions in terms of time and convenience, and SdFFF and ICP–AES can then be used for analysis of the individual GSF fractions. Detailed information on particle-size distribution and metal concentration can be obtained from SdFFF and ICP–AES, respectively. This information could then be useful in determining the source of contamination and/or the mechanism of particle formation.

Fly ash frequently contains submicron-sized particles with densities different from the average value. These particles can contaminate the GSF fractions and interfere with size analysis by Sd/StFFF. Separation of the submicron-sized particles might be necessary (e.g. by filtration) to facilitate GSF fractionation. For some samples with broad density distributions density classification [12] might be required before GSF fractionation. This enables GSF fractionation to be based purely upon size.

ICP–AES analysis of the GSF fractions showed the most abundant element in fly ash was Ca, followed by Si, and then by Mg but, interestingly, no specific correlations were found between the trace-element concentrations and particle size. Therefore, further studies of different types of fly ash sample are needed in order to obtain detailed information on patterns according to particle size.

Acknowledgements This work was supported by Grant 1999-2-124-001-5 of the Interdisciplinary Research Program, Korean Science and Engineering Foundation (KOSEF). The authors thank Dr Y.S. Chang, School of Environmental Engineering, Pohang University of Science and Technology, for providing the fly ash samples.

References

- Taylor D (1999) *Environ Health Perspect* 107:A404–A409
- Rand T, Haukohl J, Marxen U (2000) World Bank Technical Paper, No 462, World Bank, Washington DC
- Natusch DFS, Wallace JR, Evans CA (1974) *Science* 183:202–204
- Graff KA, Caldwell KD, Myers MN, Giddings JC (1984) *Fuel* 63:621–626
- Ghosal S, Self SA (1995) *Fuel* 74:522–529
- Kaupp H, Towara J, McLachlan MS (1994) *Atmos Environ* 28:585–593
- Kurokawa Y, Takahiko M, Matayoshi N, Satoshi T, Kazumi F (1998) *Chemosphere* 37:2161–2171
- Pistikopoulos P, Wortham HM, Gomes L, Masclet-Beyne S, Bon Nguyen E, Masclet PA, Mouvier G (1990) *Atmos Environ* 24A:2573–2584
- Conzemius RJ, Welcomer TD, Svec HJ (1984) *Environ Sci Technol* 18:12–18
- Furuya K, Miyajima Y, Chiba T, Kikuchi T (1987) *Environ Sci Technol* 21:898–903
- Ghosal S (1993) Ph. D. Thesis, Stanford University, USA
- Kim WS, Lee DW, Lee S (2002) *Anal Chem* 74:848–855
- Wiesner MR, Grant MC, Hutchins SR (1996) *Environ Sci Technol* 30:3184–3191
- Grout H, Tarquis AM, Wiesner MR (1998) *Environ Sci Technol* 32:1176–1182
- Strand M, Pagels J, Szpila A, Gudmundsson A, Swietlicki E, Bohgard M, Sanati M (2002) *Energy Fuels* 16:1499–1506
- Shi JP, Mark D, Harrison RM (2000) *Environ Sci Technol* 34:748–755
- Kim WS, Kim SH, Lee DW, Lee S, Lim CS, Ryu JH (2001) *Environ Sci Technol* 35:1005–1012
- Noble CA, Prather KA (2000) *Mass Spectrom Rev* 19:248–274
- Reents WD, Schabel MJ (2001) *Anal Chem* 73:5403–5414
- Norton GA, Markuszewski R, Shanks HR (1986) *Environ Sci Technol* 20:409–413
- Rincon JM, Romero M, Boccaccini AR (1999) *J Mater Sci* 34:4413–4423
- Phillies GDJ (1990) *Anal Chem* 62:1049A–1057A
- Barth HG, Sun ST (1995) *Anal Chem* 67:257R–272R
- Lee S, Rao SP, Moon MH, Giddings JC (1996) *Anal Chem* 68:1545–1549
- Kim WS, Park YH, Shin JY, Lee DW, Lee S (1999) *Anal Chem* 71:3265–3272
- Giddings JC (1995) *Anal Chem* 67:592A–598A
- Giddings JC (1993) *Science* 260:1456–1465
- Giddings JC, Moon MH (1997) *J Microcolumn Sep* 9:565–570
- Koch T, Giddings JC (1986) *Anal Chem* 58:994–997
- Caldwell KD, Cheng ZQ, Hradecky P, Giddings JC (1984) *Cell Biophys* 6:233–251
- Moon MH, Kang D, Lee DW, Chang YS (2001) *Anal Chem* 19:307–319

32. Dondi F, Contado C, Blo G, Martin SG (1998) *Chromatographia* 48:643–654
33. Moon MH, Kang D, Lim H, Oh JE, Chang YS (2002) *Environ Sci Technol* 36:4416–4423
34. Williams PS, Giddings JC (1987) *Anal Chem* 59:2038–2044
35. Yang FJF, Myers MN, Giddings JC (1974) *Anal Chem* 46:1924–1930
36. Myers MN, Giddings JC (1982) *Anal Chem* 54:2284–2289
37. Giddings JC, Moon MH, Williams PS, Myers MN (1991) *Anal Chem* 63:1366–1372
38. Springston SR, Myers MN, Giddings JC (1987) *Anal Chem* 59:344–350
39. Bódog I, Polyák K, Csikós-Hartyányi Z, Hlavay J (1996) *Microchem J* 54:320–330
40. Smith RD, Campbell JA, Nielson KK (1979) *Environ Sci Technol* 13:553–558